Available online at www.sciencedirect.com
SCIENCE DIRECT®
Proceedings of the Combustion Institute 30 (2005) 2745–2753
Proceedings of the Combustion Institute
www.elsevier.com/locate/proci

Modeling autoignition in non-premixed turbulent combustion using a stochastic flamelet approach

Guillaume Blanquart*, Heinz Pitsch

Department of Mechanical Engineering, Stanford University, Stanford, CA 94305, USA

Abstract

In this paper, a stochastic flamelet approach is used to model autoignition in an initially non-premixed medium in isotropic and decaying turbulence, using a one-step irreversible reaction. This configuration corresponds to the DNS data from Sreedhara and Lakshmisha [Proc. Combust. Inst. 29 (2002) 2069]. The system can be described by the flamelet equations for the temperature and fuel mass fraction, where the scalar dissipation rate appears as a stochastic parameter. In a turbulent flow, fluctuations of this scalar have a strong impact on autoignition. Assuming a log normal distribution, a stochastic differential equation (SDE) can be derived for the scalar dissipation rate. The decay rate of the mean dissipation rate is taken from the DNS. The DNS data suggest that the normalized variance is close to unity but depends upon the Reynolds number. The flamelet equations for the temperature and fuel mass fraction, and the stochastic differential equation are coupled and solved numerically. The effects of the turbulence are discussed, and the results are compared with the DNS database. The model reproduces the conditional mean temperature profiles and the ignition delay times with good accuracy.

1. Introduction

Substantial research efforts are presently devoted to improving the performance of automotive engines. Most engines (spark-ignition and diesel engines) show a trade-off between efficiency and low emissions. Therefore, new concepts such as homogeneous-charge compression-ignition (HCCI) engines have been developed. In both diesel and HCCI engines, local inhomogeneities in the flow field play a key role during the autoignition process. These inhomogeneities manifest in the scalar dissipation rate, which in a diesel engine is very high after start of injection, but strongly decreases with time due to the turbulent mixing process. This unsteady development of the scalar dissipation rate characterizes the autoignition process. In HCCI engines, mixture inhomogeneities are not as strong, but are often deliberately enforced to control the heat release rate. With a better understanding of the autoignition process, more advanced control strategies might be possible. The present work intends to provide a model that accounts for the effects of these local inhomogeneities, mixing, and mixing rate fluctuations on autoignition.

Many studies have been performed to investigate the effect of mixing rate fluctuations on autoignition in non-premixed turbulent media.

* Corresponding author. Fax: +1 650 725 7834.
E-mail address: gblanq@stanford.edu (G. Blanquart).

1540-7489/$ - see front matter © 2004 The Combustion Institute. Published by Elsevier Inc. All rights reserved.
doi:10.1016/j.proci.2004.08.261

These involve 3*D* isotropic decaying turbulence [1,2], counterflow diffusion flames with strain rate oscillations [3,4], 2*D* turbulent mixing layers [5], 2*D* turbulent non-homogeneous mixtures [6], and others. With these direct numerical simulations (DNS), the main features of autoignition problems have been investigated. From these studies, it has been found that the scalar dissipation rate plays a very important role in the autoignition process, and that ignition spots appear where two conditions are satisfied: the mixture fraction is close to the most reactive value Z_{MR}, and the scalar dissipation rate is low.

However, such computations are very expensive in terms of resources and time. Furthermore, complex geometries certainly cannot be considered in DNS. Several methods have been developed to model autoignition in non-premixed turbulent media. The conditional moment closure model (CMC) [7] has first been used by Baritaud and co-workers [8] to model autoignition. Similar to Linan and Crespo [9], they found that the most reactive mixture fraction during autoignition is different from the stoichiometric mixture fraction. In a more recent work, Sreedhara and Lakshmisha [10] used both first and second order conditional moment closure to model autoignition. They found that these two closure methods yield qualitatively similar predictions of the temperature profile. This is a surprising result, since it has been found in other studies [4,11] that mixing rate fluctuations are very important for the description of autoignition. In conditional moment closure, these are not present in the first order model, but would appear in the second order modeling formulation. A possible reason for the insensitivity of the modeling order is that second order modeling has been applied only for the chemical source term and not for the higher order mixing terms. Hence, fluctuations in the dissipation rate were not being accounted for. For the same reason, the temporal change of the conditional temperature during autoignition is too fast compared with the DNS data in these simulations.

The flamelet approach [12,13] has been used by Pitsch et al. [11,14,15] for predictions of autoignition under diesel engine conditions. It has been shown that fluctuations of the scalar dissipation rate can substantially influence ignition delay times [11]. The influence of mixing rate, and particularly scalar dissipation rate fluctuations has been studied in the past, mainly in the context of flame extinction [16]. However, in an unsteady environment encountered for instance in a diesel engine where the mean scalar dissipation rate decays strongly with time, it remains an open question whether the fluctuations of the scalar dissipation rate lead to an increase or a decrease in the autoignition delay time.

In this study, we will investigate and model the influence of turbulent fluctuations of the scalar dissipation rate in non-premixed combustion problems. The configuration considered here corresponds to a 3*D* non-premixed medium in isotropic and decaying turbulence. This case has been chosen, since it represents the time decaying scalar dissipation rate typically encountered in engines. We will first present the unsteady flamelet equations for a non-premixed system evolving by a one-step chemical reaction. Based on this assumption, the system will be simplified to a set of two partial differential equations. Then, we will establish a stochastic differential equation (SDE) for the scalar dissipation rate, and we will discuss the mean behavior of this parameter. Numerical solutions will be compared with DNS data from Sreedhara and Lakshmisha [1,2], and the sensitivity of the results on the model parameters will be investigated.

2. Flamelet equations

The time evolution of the species mass fractions and the temperature are modeled using the unsteady flamelet equations. This method has been found to be very successful in handling detailed chemistry and predicting pollutant formation. Here, to compare with DNS results by Sreedhara and Lakshmisha [1,2], the flamelet equations will be formulated for a one-step irreversible reaction.

We consider a one-step irreversible reaction of the form $\nu_F F + \nu_O O \rightarrow \nu_P P$, where F, O, and P are the fuel, the oxidizer, and the products, respectively. For two streams, one with fuel at a mass fraction of $Y_{F,1}$ (subscript 1) and one with oxidizer at a mass fraction of $Y_{O,2}$ (subscript 2), the mixture fraction Z is defined by

$$Z = \frac{\hat{\nu} Y_F - Y_O + Y_{O,2}}{\hat{\nu} Y_{F,1} + Y_{O,2}}, \tag{1}$$

where $\hat{\nu} = \nu_O W_O / \nu_F W_F$ is the stoichiometric mass ratio.

Under this assumption, the flamelet equations for the evolution of the temperature and the species mass fractions are given by the following equations:

$$\frac{\partial T}{\partial t} - \frac{\chi}{2}\frac{\partial^2 T}{\partial Z^2} - \frac{Q}{c_p}\omega - \frac{1}{\rho c_p}\frac{\partial p}{\partial t} = 0, \tag{2}$$

$$\frac{\partial Y_i}{\partial t} - \frac{\chi}{2}\frac{\partial^2 Y_i}{\partial Z^2} + \nu_i W_i \omega = 0. \tag{3}$$

Here, ν_i are the stoichiometric coefficients, W_i are the molecular weights, $Q = -\sum_i \nu_i W_i h_i$ is the heat release of the reaction, c_p is the specific heat capacity at constant pressure, ρ is the local density, p is the background pressure, and $\chi = 2D(\nabla Z)^2$ the scalar dissipation rate. Finally, the reaction rate per unit mass is expressed as

$$\omega = \rho \frac{Y_F}{W_F} \frac{Y_O}{W_O} A \exp\left(-\frac{E}{RT}\right), \quad (4)$$

where A is the frequency factor, E is the activation energy, and R is the universal gas constant.

Since the product mass fraction is not used in the chemical source term expression, Eq. (3) does not need to be solved for Y_P. The flamelet equations can be further simplified by considering a coupling function that comes from the definition of the mixture fraction Eq. (1).

The system of equations can now be reduced to only two equations: the temperature equation Eq. (2), and the fuel mass fraction equation Eq. (3). Since these two equations describe the local instantaneous development of an ignition kernel, the scalar dissipation rate χ appears as an external random fluctuating parameter, which has to be provided separately. The fluctuating scalar dissipation rate describes the influence of turbulent mixing on the ignition kernel.

3. Modeling of autoignition in decaying isotropic turbulence

The configuration considered here corresponds to the DNS of Sreedhara and Lakshmisha [1,2] for a non-premixed medium in isotropic decaying turbulence. The domain is a $3D$ box of a constant total mass at constant volume. As mixing proceeds with time, ignition occurs, and spots of high temperature are formed. While the local temperature increases, the background pressure also increases, which further accelerates the reaction progress.

We will first provide a model for the turbulent fluctuations of the scalar dissipation rate around its mean value in mixture fraction space. Thereafter, for the particular configuration of $3D$ isotropic decaying turbulence, the mean scalar dissipation rate as well as the pressure rise will be modeled. In a general application of the model, the background pressure and the mean scalar dissipation rate will be computed from the solution of the flow field.

3.1. Modeling the fluctuations of the scalar dissipation rate

3.1.1. General stochastic differential equation

To represent the fluctuations of the scalar dissipation rate around a mean value, we use a stochastic differential equation (SDE). It is well known that a reasonable approximation for the pdf of the scalar dissipation rate is a log-normal distribution [17]

$$P(\chi, t) = \frac{1}{\chi\sigma\sqrt{2\pi}} \exp\left(-\frac{(\ln\chi - \mu)^2}{2\sigma^2}\right) \quad (5)$$

with

$$\langle\chi\rangle = \exp(\mu + \tfrac{1}{2}\sigma^2), \quad (6)$$

$$\frac{\langle\chi''^2\rangle}{\langle\chi\rangle^2} = \exp(\sigma^2) - 1, \quad (7)$$

where μ and σ are the mean and the variance of the log-normal distribution. This assumption has been confirmed by Yeung et al. [18] who compared DNS data of the logarithm of the scalar dissipation rate for isotropic turbulence to a Gaussian distribution with good agreement. At a fixed Schmidt number (here $Sc = 0.58$), the variance of the logarithm σ is assumed to depend only on the Reynolds number. The DNS data [1] provide the ratio of the variance over the mean $\langle\chi''^2\rangle/\langle\chi\rangle^2$, from which the value for σ can be found. For other configurations, this value can be deduced from the turbulent Reynolds number [19].

We now want to write an SDE for χ such that the resulting probability density function is given by the above log-normal distribution. Using Ito's representation, the SDE has the following form [20]

$$\mathrm{d}\chi = A\,\mathrm{d}t + B\,\mathrm{d}W \quad (8)$$

where $A(\chi, t)$ is the drift coefficient, $B(\chi, t)$ is the diffusion coefficient, and $W(t)$ is the Wiener process. The probability density function $P(\chi, t)$ given by Eq. (5) is the solution to the forward equation also known as the Fokker–Plank equation

$$\frac{\partial P}{\partial t} - \frac{1}{2}\frac{\partial^2}{\partial\chi^2}(B^2 P) + \frac{\partial}{\partial\chi}(AP) = 0. \quad (9)$$

Comparing the solution of Eq. (9) with Eq. (5), the unknown coefficients A and B can be determined resulting in

$$\mathrm{d}\chi = -\left(\ln\left(\frac{\chi}{\langle\chi\rangle}\right) - \frac{1}{2}\sigma^2 - \frac{S_{\langle\chi\rangle}}{\langle\chi\rangle}T\right)\chi\frac{\mathrm{d}t}{T} + \sqrt{\frac{2}{T}}\sigma\chi\,\mathrm{d}W, \quad (10)$$

where $\langle\chi\rangle$ is a prescribed average scalar dissipation rate obtained from the DNS data, $S_{\langle\chi\rangle} = \mathrm{d}\langle\chi\rangle/\mathrm{d}t$ accounts for the change in the mean scalar dissipation rate, and T is the scalar time scale, which will be defined below.

3.1.2. Spatial correlation

It has been found from experimental measurements [21] and DNS computations [18] that the scalar dissipation rate is correlated in space. However, Eq. (10) in its present form is a one point equation whose solution is uncorrelated in mixture fraction space. To represent the spatial correlation of χ, we create smoothed white noise [22] according to

$$\mathrm{d}W_s(Z) = \frac{1}{||k||}\int_{-\Delta Z/2}^{\Delta Z/2} k(Z')\,\mathrm{d}W_{uc}(Z + Z')\,\mathrm{d}Z', \quad (11)$$

and we solve Eq. (10) as a function of Z with $\mathrm{d}W = \mathrm{d}W_s$, where $\mathrm{d}W_s$ is the smoothed white

noise, dW_{uc} is the original uncorrelated white noise, k is a kernel function, and $||k|| = \sqrt{\int_R k^2(Z')\,dZ'}$ its L^2 norm. For the kernel, we should use a C^∞ function with a compact support $[-\Delta Z/2, \Delta Z/2]$. However, since we will discretize the kernel function, the requirement of compact support can be relaxed, and we use a polynomial function of the form

$$k(Z') = \tfrac{1}{16}\Delta Z^4 - \tfrac{1}{2}\Delta Z^2 Z'^2 + Z'^4. \quad (12)$$

The initial scalar dissipation rate field has to be created with the same spatial correlation as the white noise.

The correlation in mixture fraction space ΔZ corresponds to the characteristic mixture fraction fluctuation for an appropriate correlation length scale of the scalar dissipation rate. This correlation length l_c has been found from DNS [18] and experiments [21] to be much smaller than the integral length scale of the scalar. We can distinguish between two possible situations. For sufficiently high Reynolds number, the Taylor scale λ is a reasonable choice for l_c, as λ can be found in the vicinity of the peak of the dissipation spectrum over a large range of Reynolds numbers. However, for the present DNS, λ is not the appropriate scale. Because of the relatively low Reynolds number of the DNS, the Taylor scale is of the order of the integral scale, and hence does not represent the correlation length of dissipation. In this case, the Kolmogorov scale can be used for l_c, since this certainly is a lower bound for the correlation length scale.

Using Kolmogorov's scaling for both the velocity and the scalar field in the situation of high Reynolds number, we can write the correlation length in mixture fraction space ΔZ_λ as

$$\Delta Z_\lambda = \left(\chi \frac{\left(\lambda^2 l_t\right)^{1/3}}{u'}\right)^{1/2}, \quad (13)$$

where l_t is the integral length scale, and u' is the large scale velocity fluctuation. This form of ΔZ has to be used in applications of the model in engine simulations. However, for the present DNS, we use the following definition based on the Kolmogorov scale:

$$\Delta Z_\eta = \eta\sqrt{\frac{\chi}{2D}}, \quad (14)$$

where $\chi(Z,t)$ is the instantaneous local scalar dissipation rate. The sensitivity of the results to the choice of ΔZ is discussed below.

3.2. Modeling the configuration

3.2.1. Imposed mean scalar dissipation rate

Writing Eq. (10) for a given value of the mixture fraction, the conditionally averaged scalar dissipation rate $\langle\chi|Z\rangle$ appears as an external parameter. Hence, we have to provide the conditional mean value as a function of time and mixture fraction $\langle\chi|Z\rangle(Z,t)$. In a general application of the model, this conditional mean value will be deduced from the solution of the flow field, and no further modeling of the mean scalar dissipation rate will be required.

For decaying isotropic turbulence, it is well known that the decay of the variance of a passive scalar follows a power law. Therefore, we can write the variance of the mixture fraction as

$$\frac{\langle Z''^2\rangle}{\langle Z_0''^2\rangle} = \left(1 + \frac{t}{t_0}\right)^{-m}, \quad (15)$$

where the exponent m has been found from DNS simulation and experimental results [23] to depend on the ratio $(L/L_Z)_0$ of the initial integral length scale of the velocity and scalar field. The DNS data [1] provide the ratio $(L/L_Z)_0 = 1.35$, for which it is found from Mell et al. [23] that $m = 2.46$. Then, to model $\langle\chi\rangle$, we use the following expression:

$$\langle\chi\rangle(t) = \chi_0\left(1 + \frac{t}{t_0}\right)^{-m-1}, \quad (16)$$

which follows from the assumption of isotropic turbulence.

With these expressions, we can define the scalar time scale T appearing in Eq. (10) as

$$T = \frac{\langle Z''^2\rangle}{\langle\chi\rangle} = \frac{t + t_0}{m}. \quad (17)$$

We also need to impose $\langle\chi|Z\rangle$ as a function of the mixture fraction. We assume that the conditionally averaged scalar dissipation rate has the following form:

$$\langle\chi|Z\rangle(Z,t) = 4\chi_{\max}(t)Z(1-Z). \quad (18)$$

This expression has been observed to fit the DNS data very well. Furthermore, this expression is more accurate close to the stoichiometric mixture fraction than for instance the expression from a counterflow [12]. The relation between χ_0 and $\chi_{\max}$ comes from

$$\langle\chi\rangle(t) = \int \langle\chi|Z\rangle(Z,t)P(Z)\,dZ, \quad (19)$$

which gives as the final expression for the imposed mean scalar dissipation rate

$$\langle\chi|Z\rangle(Z,t) = \frac{\chi_0 Z(1-Z)}{\langle Z\rangle(1-\langle Z\rangle) - \langle Z''^2\rangle}\left(1 + \frac{t}{t_0}\right)^{-m-1}. \quad (20)$$

3.2.2. Pressure modeling

Assuming that the simulation is performed in the low Mach number limit, the background pressure p is homogeneous, and hence will be determined as the box average

$$p = \rho_0 R \left(\int_Z \frac{W(Z)}{T(Z)} P(Z)\, \mathrm{d}Z \right)^{-1}, \tag{21}$$

where $W(Z)$ and $T(Z)$ are the molecular weight of the mixture and the local temperature, respectively. $P(Z)$ represents the probability density function of Z. We assume that the mixture fraction pdf is a β-function depending on the mean and the variance of the mixture fraction. For the present case, the mean mixture fraction is constant at $\langle Z \rangle = Z_{st} = 0.0621$ corresponding to an *n*-heptane and air mixture. The expression for the variance of the mixture fraction has been described earlier. The mixture fraction pdf changes with time due to mixing, whereas the temperature changes due to ignition. As a consequence, the background pressure is not constant in time.

The local density is then given by

$$\rho = \frac{pW(Z)}{RT(Z)}. \tag{22}$$

4. Numerical method

The stochastic differential Eq. (10) can be solved independently from the flamelet Eqs. (2) and (3). To solve the SDE, we use a second order Milshtein scheme [24]. The two coupled flamelet equations are solved using a second order Crank–Nicholson scheme with an iterative Newton solver.

Since we are using a stochastic approach, a large number of realizations for different noise paths are computed. Here, each simulation has been done with 4000 realizations. Then, we take the conditional ensemble average of the main variables at a constant time and mixture fraction. We are especially interested in the most reactive mixture fraction [9,8] $Z_{MR} = 0.12$, where the first spots of high temperature appear.

Following its definition from Eq. (21), the background pressure is different for every single realization. Rather than solving each flamelet with the pressure determined from Eq. (21), all flamelets are solved with the average pressure over all flamelets.

The parameters that have been used are taken from the DNS data of Sreedhara and Lakshmisha [1,2]. Different configurations, called runs *A*, *B*, and *C*, have been considered. The only difference between these three cases is the variation of the eddy turnover time, which is equivalent to the variation of the Reynolds number. The time scale t_0 and the variance σ are the only variables influenced by the eddy turnover time. The initial mean scalar dissipation rate as well as the initial integral length scale are constant for the three runs at $\chi_0 = 3.96\ \mathrm{s}^{-1}$ and $l_t = 0.57$ mm, respectively.

Table 1
Model parameters from the DNS data [1] for runs *A*, *B*, and *C*

Run	Re_L	σ	t_0 (ms)	u' (mm/s)
A	38.5	0.8	50	20
B	57.8	1.1	33	30
C	77.0	1.4	25	40

5. Numerical results

Numerical solutions have been computed for the three runs (*A*, *B*, and *C*). The different parameters used for these computations are summarized in Table 1. Figure 1 shows a single realization of the simulation in three different views. Figure 1A shows the temporal evolution of the scalar dissipation rate at the most reactive mixture fraction for a given noise path and is compared with the imposed mean scalar dissipation rate. The mean starts at a value high enough to prevent ignition, but according to Eq. (20), the value decreases strongly with time. This behavior closely resembles the dissipation rate history in a diesel engine [11]. The instantaneous realization essentially follows this trend, but shows large departures from the mean values. The evolution of the temperature with the scalar dissipation rate for this case is

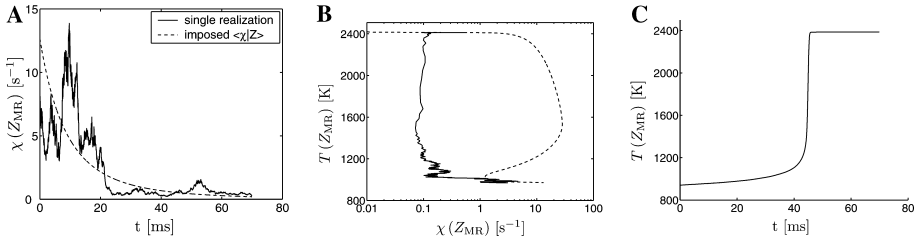

Fig. 1. Effect of the dissipation rate on the temperature evolution for one single realization at most reactive mixture fraction; (A) time evolution of χ (solid line) compared to the imposed mean dissipation rate (dashed line); (B) temperature evolution with respect to χ (solid line) compared to the S-shaped curve (dashed line); (C) time evolution of the temperature.

shown in Fig. 1B. For a comparison, the steady state solutions of the flamelet equations, given by the so-called S-shaped curve are also shown in this figure. Ignition can only occur, when the scalar dissipation rate decreases below the lower turning point of this curve, which for the present case occurs at around $t = 20$ ms. Even thereafter, it still takes approximately 20 ms for the kernel to ignite. The temporal evolution of the temperature is given in Fig. 1C. Ignition occurs at approximately $t = 45$ ms. This is much later than the homogeneous ignition delay time, which is $\tau_{ig} = 30$ ms. It is interesting to note that although the scalar dissipation rate has such a strong influence, the random variations of this quantity are not visibly present in the temperature. Once the temperature is approximately above 1200 K, the final temperature increase occurs nearly instantaneously.

The results of the present simulations are compared with DNS data for all three cases in Fig. 2. Conditional averages of the temperature at the most reactive mixture fraction ($Z_{MR} = 0.12$) are shown. In addition, the temperature evolution for the homogeneous case is also shown. It is obvious that the final temperature obtained from the model and the DNS data is not the same. The final temperature of the model simulations corresponds to the adiabatic flame temperature at the specific mixture fraction, which, in the absence of differential diffusion effects, should be the upper limit of the temperature. It appears that the very sudden temperature increase during the autoignition process leads to numerical overshoots in the DNS data leading to locally overestimated temperature, which slowly decays towards the equilibrium value. However, this is without consequence for the present study, since we are interested only in the actual ignition process.

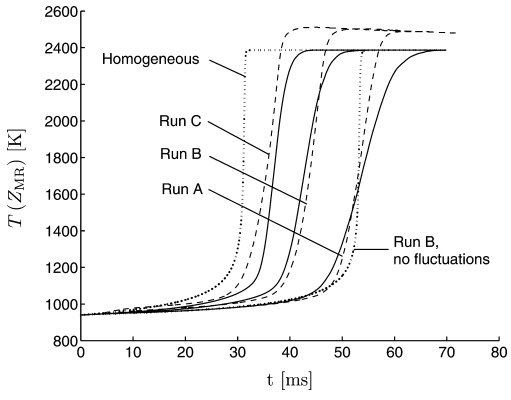

Fig. 2. Comparison of the predicted evolution of the conditional average of the temperature at the most reactive mixture fraction $Z_{MR} = 0.12$ (solid lines) with DNS data (dashed lines) during autoignition.

Regarding the ignition delay times (Fig. 2), the comparison with the DNS data shows good agreement for all three test cases. The slope of the temperature near the time of ignition is well represented for the lower Reynolds number cases, but tends to be overpredicted for higher Reynolds number. However, for both DNS and the model results, the slope of the temperature near the time of ignition is much lower than for the homogeneous case and the case without scalar dissipation rate fluctuations. The main reason for this is that because of the fluctuations of χ, each ignition kernel has a different ignition delay time. As a consequence, the temperature average spreads over a much longer period. This also leads to an ambiguity in a definition of the ignition delay time in a turbulent environment, where possible definitions could be based on the single realizations or the mean temperature development.

The comparison with the homogeneous case (for an identical mixture), which ignites at approximately $\tau_{ig} = 30$ ms, demonstrates the strong influence of the scalar dissipation rate. Figure 2 also shows results of a simulation, where no fluctuations of the scalar dissipation rate have been considered. This simulation has been carried out using the same parameters as for run B, but with $\sigma = 0$. The comparison of this simulation with the result for run B highlights the strong effect of mixing rate fluctuations on the autoignition process. In particular, this result shows that in the present environment of a decaying scalar dissipation rate, which is typical for diesel engines, fluctuations of the mixing rate lead to lower ignition delay times. The reason is in the very strong non-linearity around the lower turning point of the scalar dissipation rate. As long as the scalar dissipation rate is above this limit, positive fluctuations of the scalar dissipation rate are of insignificant consequence. However, a decrease in the scalar dissipation below this limit may lead to ignition, even if the mean value is still above this limit. Note, however, that as shown in Fig. 1, even if the local value of the scalar dissipation rate decreases below the ignition limit, autoignition is still not instantaneous. This means that short excursions below the ignition limit are possible without much influence.

Because the correlation length l_c (or ΔZ in mixture fraction space) has to be specified in the model, it is of interest to investigate its influence on the solution. In the following, we will consider two limiting cases. When the correlation length tends to zero, random scalar dissipation rate fluctuations are locally independent. Then, there is always a chance that one of the points has a low dissipation rate, which would allow for autoignition. The mixture will ignite as soon as only one of the neighboring points ignites. As a consequence, ignition delay times will be lower and not as widely distributed as in the case of high

correlation. When the correlation length is very high, temperature variations due to mixing rate fluctuations are the same for all considered points. The probability of finding at least one low value of the dissipation rate for this case is much lower, and the average ignition delay time will hence be longer. It has been found that the correlation should be weaker than predicted by Eq. (14). A possible reason could be that the simple scaling arguments used might not be accurate enough to determine the correlation length in mixture fraction space. However, for high Reynolds number, this value is assumed to be much smaller, so that the results might become more independent from this quantity.

6. Parameter analysis

The model involves three parameters, which represent the turbulence and mixing state of the considered case. In an engine, these would, for instance, be determined by the engine speed and the injection process, which influence the turbulent kinetic energy and the integral time scale. The three parameters appearing in the stochastic differential equation for the scalar dissipation rate are: σ, t_0, and χ_0. Their values are determined by the initial turbulence: χ_0 corresponds to the initial mean value of the scalar dissipation rate, t_0 to the decay rate, and σ represents the fluctuations of the scalar dissipation rate. It is interesting to note that all these quantities relate to the scalar field and do not have a length scale. However, since the time scale t_0 scales as l_t/u', and the scalar dissipation rate scales as $\chi \sim Z''^2 u'/l_t$, these quantities will be influenced by changing u' or l_t individually.

Figure 3 shows the effect of these three parameters on the ignition delay time itself and on its probability distribution. An increase either of the initial dissipation rate χ_0 or of the decay time t_0 leads to an increase of the ignition delay time. Due to the increased dissipation, it takes longer to reach the point where the dissipation rate is low enough for the mixture to ignite. Hence, the influence of these parameters depends on the mean value of the dissipation rate. It can also be noticed that these changes have an effect on the width of the probability density function of the ignition delay time. As the ignition delay time decreases, the fluctuations of χ have a smaller and smaller impact on the solution. Therefore, the width of the pdf becomes smaller.

The third parameter σ is assumed to depend only on the Reynolds number [19] and the dependence is relatively weak. As discussed earlier, because of the strong non-linearity around the lower turning point of the S-shaped curve, an increased variance in the fluctuations of χ leads to earlier ignition in average. Similarly, if the fluctuations of χ are larger, then the fluctuations of the ignition delay time are expected to be larger. However, since the mean ignition delay time simultaneously approaches the homogeneous ignition delay time, fluctuations of τ_{ig} have to become smaller. These two opposite effects balance each other, and the width of the pdf is nearly constant when σ is changed.

7. Conclusion

In the present study, we have presented an unsteady stochastic flamelet model to describe and analyze autoignition in a turbulent environment for conditions typically encountered in internal combustion engines. Considering a one-step global reaction, the flamelet equations for the temperature and the fuel mass fraction have been coupled with a stochastic differential equation for the scalar dissipation rate. For 3D isotropic homogeneous and decaying turbulence, the stochastic evolution of the conditionally averaged scalar dissipation rate has been modeled as a function of time and mixture fraction. Simulation results have been compared with DNS data, and

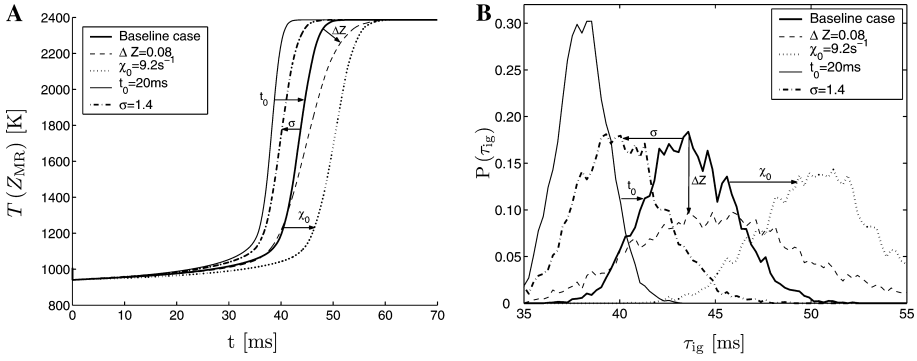

Fig. 3. Influence of parameter variations on autoignition: baseline case B with constant $\Delta Z = 0.02$, $\sigma = 1.1$, $\chi_0 = 4.6\ s^{-1}$; (A) conditionally averaged temperature at most reactive mixture fraction; (B) pdf of ignition delay time. Arrows are in the direction of increasing parameter.

the effects of different model parameters have been discussed.

The comparison of the simulation results with DNS data for three different cases shows good agreement. The analysis shows that the fluctuations of the scalar dissipation rate χ are very important. It has been found that the ignition delay time depends strongly upon the variance parameter of χ. In particular, these fluctuations lead to shorter ignition delay times compared to cases without fluctuations. These fluctuations are also responsible for a smaller change of the mean temperature near the time of ignition.

The model provides a good framework to incorporate the influence of the scalar dissipation rate and its fluctuations on autoignition into engine CFD simulations, but also for fundamental studies of the influence of inhomogeneities of mixture fraction, temperature, or residual gases on autoignition, for instance in HCCI engines.

Acknowledgments

The authors gratefully acknowledge funding by the US Department of Energy within the ASCI program and the Robert Bosch Research and Development Center. We also express our gratitude to Prof. Sreedhara for making his DNS database available, and for the invaluable help he provided in interpreting the results.

References

[1] S. Sreedhara, *Studies on Autoignition in a Turbulent Nonpremixed Medium Using Direct Numerical Simulations*, Ph.D. thesis, 2002.
[2] S. Sreedhara, K.N. Lakshmisha, *Proc. Combust. Inst.* 29 (2002) 2051–2059.
[3] S.D. Mason, J.H. Chen, H.G. IM, *Proc. Combust. Inst.* 29 (2002) 1629–1636.
[4] S. Liu, J. Hewson, J.H. Chen, H. Pitsch, *Combust. Flame* 137 (2004) 320–339.
[5] E. Mastorakos, T.A. Baritaud, T.J. Poinsot, *Combust. Flame* 109 (1997) 198–223.
[6] T. Echekki, J.H. Chen, *Proc. Combust. Inst.* 29 (2002) 2061–2068.
[7] A.Y. Klimenko, R.W. Bilger, *Prog. Energy Combust. Sci.* 25 (1999) 595–687.
[8] E. Mastorakos, A.P. Da Cruz, T.A. Baritaud, T.J. Poinsot, *Combust. Sci. Technol.* 125 (1997) 243–282.
[9] A. Linan, A. Crespo, *Combust. Sci. Technol.* 14 (1976) 95–117.
[10] S. Sreedhara, K.N. Lakshmisha, *Proc. Combust. Inst.* 29 (2002) 2069–2077.
[11] H. Pitsch, H. Barths, N. Peters, SAE Paper 962057, 1996.
[12] N. Peters, *Prog. Energy Combust. Sci.* 10 (1984) 319–339.
[13] N. Peters, *Proc. Combust. Inst.* 21 (1987) 1231–1250.
[14] H. Pitsch, Y.P. Wan, N. Peters, SAE Paper 952357, 1995.
[15] Y.P. Wan, H. Pitsch, N. Peters, SAE Paper 971590, 1997.
[16] H. Pitsch, C.M. Cha, S. Fedotov, *Combust. Theory Model.* 7 (2003) 317–332.
[17] N. Peters, *Combust. Sci. Technol.* 30 (1983) 1.
[18] P. Vedula, P.K. Yeung, R.O. Fox, *J. Fluid Mech.* 433 (2001) 29.
[19] S.K. Liew, K.N.C. Bray, J.B. Moss, *Combust. Flame* 56 (1984) 199–213.
[20] F. Klebaner, *Introduction to Stochastic Calculus with Applications.* Imperial College Press, 2001, p. 87.
[21] A.N. Karpetis, R.S. Barlow, *Proc. Combust. Inst.* 29 (2002) 1929–1936.
[22] H. Holden, B. Oksendal, J. Uboe, T. Zhang, *Stochastic Partial Differential Equations.* Birkhaeuser, 1996, p. 16.
[23] W. Mell, G. Kosaly, J. Riley, *Phys. Fluids* 3 (1991) 2474–2476.
[24] G.N. Milshtein, *Theory Prob. Appl.* 19 (1974) 557–562.

Comments

E. Mastorakos, University of Cambridge, UK. Does the model include flame propagation following a localized auto-ignition spot? This phenomenon is responsible, to an extent, for the slope of the temperature rise with time.

Reply. The presented model is intended to be used as an ignition model for internal combustion engines, and would in such an application be incorporated in a combustion model. However, the present model does not account for flame propagation following an ignition spot. But flame propagation might become important once ignition has occurred. Hence it might affect the later part of the slope of the temperature rise with time, whereas the early part of the temperature rise is mainly due to random localized auto-ignition spots. This effect will be greater for the higher Reynolds number case and is hence consistent with the under-prediction of the slope of the temperature for Run C shown in Fig. 2.

•

Norbert Peters, RWTH Aachen, Germany. In previous LES simulations, you have shown that scalar dissipation rate fluctuations considerably alter the results. How does your present stochastic approach fit into the LES context?

Reply. In our previous large eddy simulations, we have shown that the resolved fluctuations of the scalar dissipation rate might strongly influence modeling results, and we have argued that although the dissipation

occurs at the smallest scales, large changes of the dissipation rate occur on the large scales. However, this does not consider the unresolved part of the dissipation rate fluctuations, and the importance of these is yet unclear. The present stochastic model can be used as a sub-filter model for the dissipation rate fluctuations and would allow modeling and assessing the influence of small scale fluctuations of the dissipation rate.